Journal of Materials Chemistry A

ROYAL SOCIETY OF CHEMISTRY

PAPER

View Article Online
View Journal | View Issue



Cite this: *J. Mater. Chem. A*, 2020, **8**, 6564

# Photocatalytic activity of 2D nanosheets of ferroelectric Dion–Jacobson compounds†

Wei Xiong,[a] Harshit Porwal,[a] Hui Luo,[ab] Vicente Araullo-Peters,[a] Jingyu Feng,[ab] Maria-Magdalena Titirici,[ab] Michael J. Reece*[a] and Joe Briscoe*[a]

Dion–Jacobson compounds have a layered perovskite structure, and a small number of them have been identified as being ferroelectric. Here, $RbBiNb_2O_7$ powders are made by conventional solid-state synthesis. The relatively large Rb ion produces an interlayer within the structure with a large spacing and weak bonding. This work shows for the first time that a polar layered perovskite can be exfoliated into 2D nanosheets using a facile and scalable method, namely liquid-phase sonication. With both 2D materials and ferroelectrics being of interest for photocatalysis, the photocatalytic performance of $RbBiNb_2O_7$ nanosheets is characterized by measuring its dye degradation rate under a solar simulator. It is demonstrated that the $RbBiNb_2O_7$ nanosheet material effectively decolourizes Rhodamine B under visible illumination even though it has a wide bandgap (3.45 eV), and that its photocatalytic activity is greatly enhanced (~4 times faster) when decorated with photodeposited Ag nanoparticles. Reducing the nanosheet size also increases the photocatalytic performance. This work demonstrates that polar 2D Dion–Jacobson phase $RbBiNb_2O_7$ is a promising candidate for photocatalytic applications. Further improvements are possible by identifying compounds with a narrower bandgap as a broad compositional window is available in this family of compounds.

Received 22nd October 2019
Accepted 31st January 2020

DOI: 10.1039/c9ta11639g

rsc.li/materials-a

## 1. Introduction

Dion–Jacobson (DJ) compounds, having the general formula of $A'A_{n-1}B_nO_{3n+1}$, form a family of layered perovskites. They consist of $n$ perovskite blocks that are made of corner sharing $BO_6$ octahedra with A-site cations in the 12-coordinate sites. These blocks are separated by layers of A′ cations. Their unique structure leads to many interesting properties, making them of interest for many applications, including for solar cells,[1,2] water splitting[3,4] and ferroelectrics.[5–7]

It is known that DJ phase materials can be exfoliated into nanosheets due to the large interlayer spacing and weak bonding of the A′ layers. M. Hojamberdiev *et al.*[3] exfoliated the centrosymmetric, non-polar, three-layer compound $CsBa_2Ta_3O_{10}$ by a sequence of steps involving nitridation–protonation–intercalation to produce nanosheets. They investigated its properties as a catalyst for water splitting. A few papers[8–13] have reported the exfoliation of layered perovskites and measured their dielectric or optoelectrical properties, for instance, T. C. Ozawa *et al.*[9] exfoliated $Li_2Eu_{0.56}Ta_2O_7$ and $K(K_{1.5}Eu_{0.5})Ta_3O_{10}$ with three-step reactions and reported their photoluminescence emission spectra; B.-W. Li *et al.*[11] exfoliated $KLa_{0.95}Nb_2O_7$ and $KLa_{0.90}Eu_{0.05}Nb_2O_7$ and measured their dielectric properties on re-assembled thin films; M. Osada *et al.*[12] exfoliated $KCa_2Nb_3O_{10}$, $KSr_2Nb_3O_{10}$ and $KSr_2Ta_3O_{10}$, and then applied the same Langmuir–Blodgett (LB) process as B.-W. Li *et al.* to prepare multi-layer thin films for dielectric characterizations. However, reports on successful exfoliation of polar/ferroelectric layered perovskites are scarce. Moreover, the few papers[14–16] that reported exfoliated nanosheets from polar parent phases, such as $SrBi_2Ta_2O_9$ and $KCa_2Na_2Nb_5O_{16}$ (0.2 C $m^{-2}$), all used complex multi-step chemical exfoliation routes like those used above. There is hence a need for a simple and scalable exfoliation method to prepare polar perovskite nanosheets.

Recently, exciting new results have emerged that demonstrate ferroelectricity in the non-centrosymmetric, polar, two-layer DJ phase $ABiNb_2O_7$ (A = Rb, Cs).[6,7] Like some simple perovskites (*e.g.* $BaTiO_3$), their spontaneous polarization originates from displacement of the A-site cations and tilting of the octahedra.[17] The spontaneous polarization of $CsBiNb_2O_7$ ($a$ = 5.4964, $b$ = 5.4223 and $c$ = 11.3704 Å) and $RbBiNb_2O_7$ ($a$ = 5.4193, $b$ = 5.3589 and $c$ = 11.2099 Å) were calculated to be around 0.438 and 0.47 C $m^{-2}$, respectively.[7] It is of great interest to investigate the potential photocatalytic properties of these highly-polar materials. The possibility of being able to produce them as nanosheets by exfoliation offers the potential to generate high-surface-area catalyst materials that have polar

[a]School of Engineering and Material Science, Materials Research Institute, Queen Mary University of London, Mile End Road, London E1 4NS, UK. E-mail: m.j.reece@qmul.ac.uk; j.briscoe@qmul.ac.uk

[b]Department of Chemical Engineering, Imperial College London, South Kensington Campus, London SW7 2AZ, UK

† Electronic supplementary information (ESI) available. See DOI: 10.1039/c9ta11639g

ferroelectric domains. Such ferroelectric polarization in layered perovskites not only enhances, but also controls photocatalytic reactions through selective redox chemistry.[18,19] Inducing selective reduction or oxidation reactions at controllable locations on 2D structures enables spatial separation of photo-excited electron–hole pairs. This can effectively reduce charge carrier recombination and thus improve photocatalytic efficiency. Another hot topic is band engineering of layered perovskite photocatalysts, which has been reviewed theoretically and experimentally.[20–22] Methods like substituting transition metal cations in the Ruddlesden–Popper phases[21] and incorporating hybrid systems such as single metal oxides/perovskites[19,21,22] are suggested to fabricate narrow bandgap catalysts.

Here we present the first demonstration of photocatalytic activity in 2D nanosheets of ferroelectric $RbBiNb_2O_7$. The material was prepared by a simple and scalable method involving sonication of powder suspensions to exfoliate nanosheets. We show that a significant enhancement of photocatalytic activity can be achieved by photodeposition of Ag nanoparticles onto the nanosheets, and that this deposition selectively occurs on polar edge sites. Furthermore, we show by size separation of the nanosheets that photocatalytic activity correlates with sheet size, with higher activity for smaller sheets.

## 2. Experimental methods

### 2.1 Solid-state synthesis

$RbBiNb_2O_7$ powder was synthesized by mixing stoichiometric amounts of $Rb_2CO_3$ (4 mass% excess to compensate for Rb loss), $Bi_2O_3$ and $Nb_2O_5$, and then calcining at 1000 °C for 4 hours in air. The product was ground and re-milled with ethanol for 24 h, then re-calcined at 1000 °C for 4 hours in air for better phase formation.

### 2.2 Exfoliation and size selection

We used a facile and scalable method to exfoliate $RbBiNb_2O_7$. This was completed in two cycles. In the first cycle, 10 g of $RbBiNb_2O_7$ powder was mixed with 100 mL of 1-methyl-2-pyrrolidone (NMP) solvent and then sonicated for 10 h using an ultrasonic processor (VCX500, Sonics). After filtering the sonicated suspension, the precipitate was mixed with fresh NMP for a second and final 10 h of sonication. A lab centrifuge (C2 series, Centurion Scientific) was used at 500 rpm and 1000 rpm to separate different sizes of nanosheets from exfoliated $RbBiNb_2O_7$ suspensions.

### 2.3 Ag photodeposition

0.3 g of exfoliated material was mixed with 15 mL of $AgNO_3$ aqueous solution (0.01 M). The solution mixture was irradiated with a UV illumination source (Hg lamp, 5.28 mW $cm^{-2}$) for 30 seconds under constant stirring. After photodeposition, the powder was centrifuged and washed with distilled water, then dried for photocatalytic measurement.

### 2.4 Characterization

X-ray diffraction of the bulk and exfoliated $RbBiNb_2O_7$ was performed using a Panalytical X'pert Pro diffractometer (Cu-$K_{\alpha 1}$ $\lambda = 1.5406$ Å). Ultraviolet-visible (Lambda 35 & Lambda 950, PerkinElmer) and Raman (inVia reflex, Renishaw) spectra were recorded for bulk and exfoliated samples. Energy-dispersive X-ray spectroscopy (EDX) on silver-decorated samples was carried out using a scanning-electron microscope (FEI, Inspect F). Transmission-electron microscopy of exfoliated samples and silver-decorated samples was carried out using a JEOL JEM-2010. Atomic force microscopy (AFM) micrographs of exfoliated nanosheets on a silicon substrate were recorded using a Bruker Dimension Icon. Photocatalytic performance was characterized using the degradation rate of Rhodamine B dye solution (initial concentration 50 ppm) in the presence of exfoliated samples using a PerkinElmer Lambda 35 UV-vis spectrophotometer. The degradation process was performed under a solar simulator (Newport, class ABB) with an intensity of 100 mW $cm^{-2}$ and an AM 1.5 filter. The specific surface area of the exfoliated samples was calculated using the Brunauer–Emmett–Teller (BET) method, and nitrogen absorption isotherm data was obtained using a gas sorption analyzer (Autosorb-IQ, Quantachrome Instruments).

## 3. Results and discussion

The Dion–Jacobson $RbBiNb_2O_7$ powder was synthesised using a conventional solid-state synthesis method, with the phase and structure confirmed by XRD and Raman analysis (Fig. S1 and S2†). In order to test its photocatalytic activity, high-surface-area powder samples are required. We investigated the possibility of preparing 2D nanosheets of $RbBiNb_2O_7$ by sonication. Unlike conventional exfoliation methods, which include multiple steps like protonation, intercalation, sonication and centrifugation, our method only requires one simple and scalable technique without the need for the addition of solvents like tetra(*n*-butyl) ammonium hydroxide (TBAOH). Transmission-electron microscopy (TEM) imaging showed that exfoliated nanosheets were produced, some of which were broken into smaller pieces (Fig. 1). This is commonly observed when exfoliating many

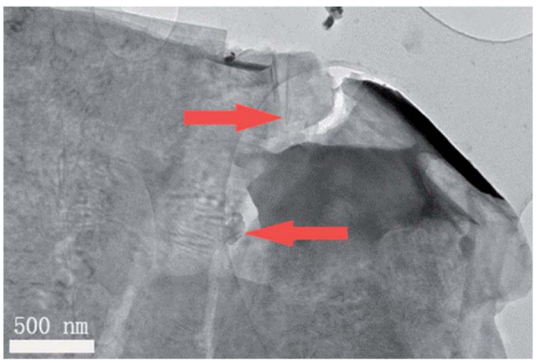


Fig. 1 TEM image of exfoliated $RbBiNb_2O_7$ nanosheets showing breakage (see arrows).

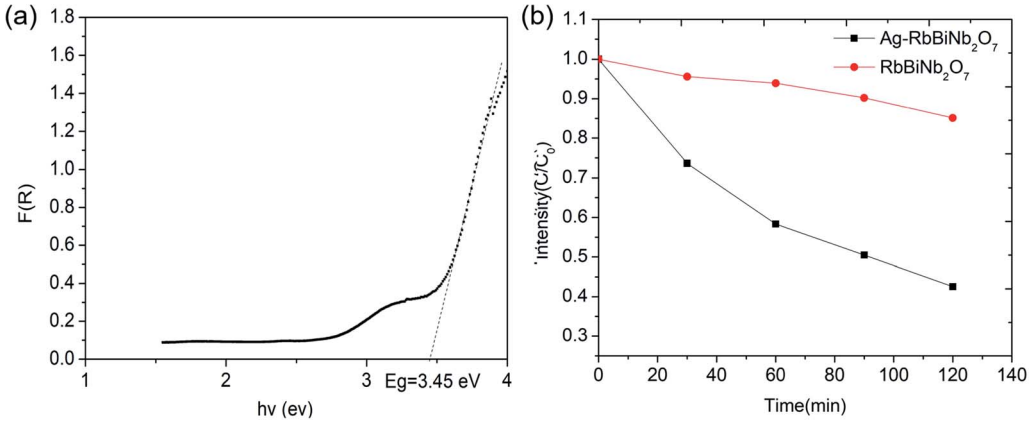


Fig. 2 (a) Kubelka–Munk function fitting of $RbBiNb_2O_7$'s diffuse reflectance spectrum; (b) photocatalytic dye decolourization performance of exfoliated $RbBiNb_2O_7$ samples with/without Ag photodeposition.

materials, including graphene.[23] For photocatalytic applications, the break-up is in fact desirable, as it increases the overall surface area of the catalyst. Calculated by the multipoint Brunauer–Emmett–Teller (BET) method, the exfoliated $RbBiNb_2O_7$ had a total specific surface area of 16.04 $m^2\ g^{-1}$ (Fig. S3†). This is much larger than the previous report for $BaTiO_3$-based powders (2.055 $m^2\ g^{-1}$).[24] AFM imaging of exfoliated nanosheets estimates their thickness to be 5–7 nm (Fig. S4†). XRD and Raman analysis (Fig. S1 and S2†) both demonstrate that no change in structure, phase or composition occurred because of the exfoliation.

The photocatalytic activity of $RbBiNb_2O_7$ was evaluated using dye degradation analysis in order to provide a standardized comparison of catalytic activity, and to facilitate comparison with previous reports. The results show that despite the wide bandgap of the DJ material, which was found to be 3.45 eV from the Kubelka–Munk transformation $\left(F(R) = \frac{(1-R)^2}{2R}, \text{ where } R \text{ is diffuse reflectance}\right)$ (Fig. 2a) of its UV/vis reflectance data, bare $RbBiNb_2O_7$ nanosheets can successfully degrade Rhodamine B dye even under visible illumination (AM 1.5, 100 mW $cm^{-2}$) (Fig. 2b). However, the rate was relatively slow, degrading by only ~13% after 2 hours. Similar results were also found for exfoliated $CsBiNb_2O_7$ (Fig. S5†), but $RbBiNb_2O_7$ will be the focus of this paper due to its reported stronger ferroelectricity. As a control experiment, Fig. S6† shows that unexfoliated $RbBiNb_2O_7$ does not degrade the RhB dye.

A large enhancement of photocatalytic activity can be achieved for ferroelectric photocatalysts using preferential photoreduction of an Ag precursor on the positively polarized surface. This has previously been demonstrated for ferroelectric $BaTiO_3$, where Ag nanoparticles were deposited on the material surface as a co-catalyst using photochemical deposition.[24] In the current study, Ag nanoparticles were similarly deposited on the $RbBiNb_2O_7$ nanosheets by photochemical deposition (Fig. 3). EDX analysis also confirms successful deposition of Ag particles on exfoliated nanosheets (Fig. S7†), which led to a large increase in the photocatalytic activity, with a 57% reduction in dye concentration after 2 hours (Fig. 2b). This enhancement stems from the metallic nanoparticles on the ferroelectric materials, which are known to enhance the effect of polarization-induced band bending at their interface and act as sinks for photogenerated electrons, which lowers the recombination rate of electron–hole pairs.[19] TEM images of Ag-deposited samples showed selective photodeposition of Ag nanoparticles (~5 nm) on edge sites (Fig. 3), which are likely to be the polar surfaces of the material as reported by other groups.[25,26] Recyclability test (see Fig. S8†) confirmed that the catalytic activity was maintained after collecting, washing and re-using the catalyst.

To further investigate the effect of the size of the nanosheets on the catalytic activity, size-separation was achieved by centrifuging the samples at 500 and then 1000 rpm. This led to two fractions with larger (500 rpm) and smaller (1000 rpm) average diameters of 333 ± 272 nm and 245 ± 162 nm respectively, measured from an average of 80 nanosheets (assuming circular shape). The full histograms, which demonstrates the size difference, can be seen in Fig. 4a and b. Both samples had similar UV/vis absorbance curves (Fig. S9†), showing that the

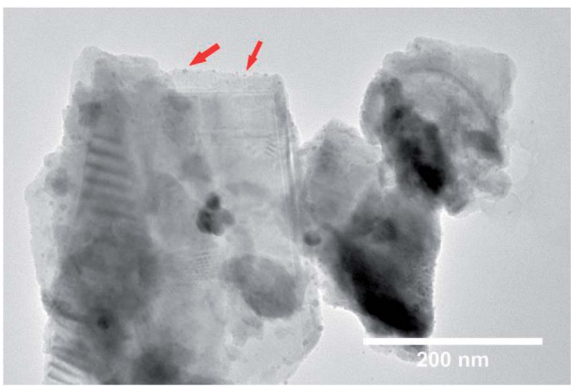


Fig. 3 TEM image of Ag particles (arrows) on the surface of exfoliated $RbBiNb_2O_7$ nanosheets. Ag nanoparticles preferentially deposit on the polar edge sites (where there is a slight contrast change), and little on the non-polar faces of the nanosheets.

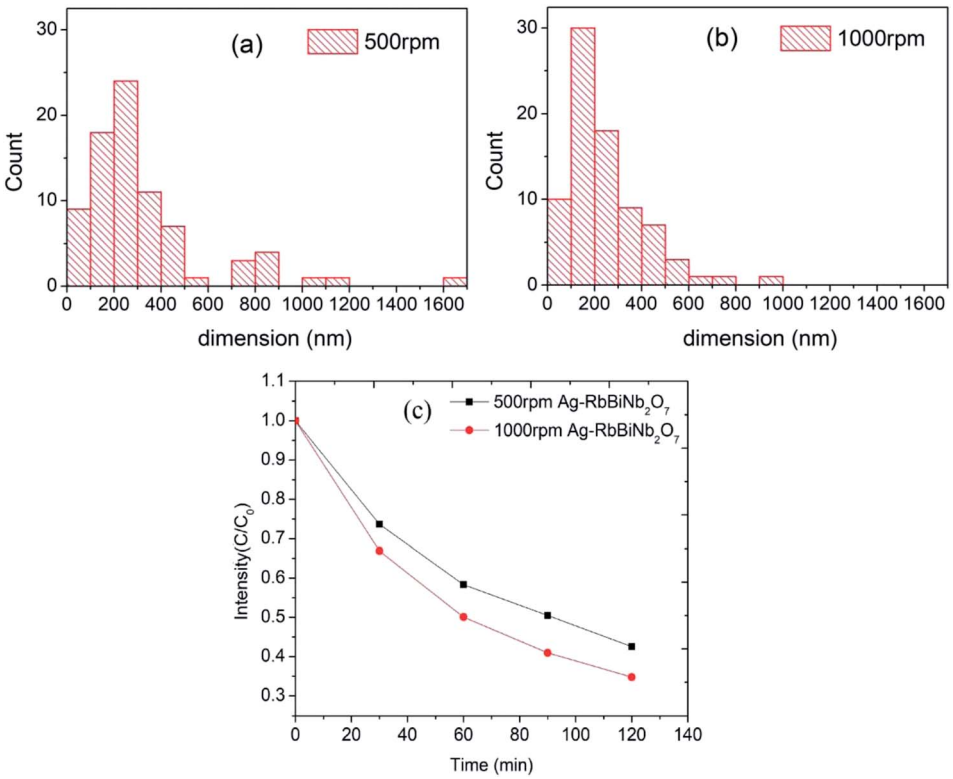


Fig. 4 Histogram of nanosheet lateral size for samples separated at: (a) 500 rpm; (b) 1000 rpm. (c) Photocatalytic dye decolorization performance of exfoliated $RbBiNb_2O_7$ samples centrifuged at 500 or 1000 rpm, with larger and smaller average diameters, respectively.

optical properties were conserved after centrifugation. The rather large standard deviation in the sizes was due to remaining unexfoliated bulk material after centrifugation, the cause of which is as follows: conventionally the product is obtained from the supernatant by going from higher to lower centrifuge speed to extract first smaller and then larger sized particles.[27] However, here we extracted the products from the precipitates in order to maximise the yield for the photocatalysis experiments. Therefore, our samples inevitably contained some large bulk material. As demonstrated by M. Buzaglo *et al.*[28] in their graphene scale-up work, for liquid-phase-sonicated and then centrifuged samples, most of the graphene products were from the precipitates and had larger size than those in the supernatant, and Raman confirmed that neither were damaged by the sonication process in terms of in-plane defects (however, there were edge defects).

Dye decolourization tests using 500 rpm and 1000 rpm samples (equal mass) demonstrated that, as expected, the Ag-decorated photocatalyst with a smaller average diameter (1000 rpm), and therefore higher surface area, had a higher photocatalytic activity than the larger diameter nanosheets (Fig. 4c). The rate constant ($k$) for dye degradation was calculated using first-order kinetics $\left(\ln\left(\frac{C}{C_0}\right) = kt\right)$ (see Fig. S10† for full details of fitting). The results are listed in Table 1 to quantify the overall photocatalytic activity. Besides the increase in surface area, the size enhancement may be particularly notable because the decrease in the size of the nanosheets led to an increase of the polar, Ag-decorated edge sites, which are likely to be the most catalytically active. This size effect therefore makes layered perovskites potentially very promising candidates for photocatalytic applications, as their dimension can be reduced to a desired level using the facile and scalable method of liquid-phase sonication.

Table 1 Rate constants of exfoliated $RbBiNb_2O_7$ samples under different conditions

| Sample | $k$ [$min^{-1}$] | $R^2$ |
|---|---|---|
| 500 rpm $RbBiNb_2O_7$ | 0.0013 | 0.96 |
| 500 rpm Ag–$RbBiNb_2O_7$ | 0.0070 | 0.97 |
| 1000 rpm Ag–$RbBiNb_2O_7$ | 0.0087 | 0.96 |

## 4. Conclusions

We show for the first time that it is possible to exfoliate a polar layered perovskite using a facile and scalable method, namely liquid-phase sonication. Nanosheets of $RbBiNb_2O_7$ can decolourize Rhodamine B under visible light, with $CsBiNb_2O_7$ also shown to have a similar photocatalytic activity (degradation rate of 6.5% per hour). A large enhancement of photocatalytic performance can be made by depositing silver nanoparticles on $RbBiNb_2O_7$ due to reduced electron–hole recombination, which increases the degradation rate by almost a factor of four. We show by TEM imaging that the Ag nanoparticles are selectively

photodeposited on the polar edge sites of the nanosheets. We compared two samples with different average size by using different centrifuge speeds and found that smaller nanosheets have better performance than larger ones as a result of their increased surface area. This makes layered perovskites promising photocatalytic materials that can be easily exfoliated into 2D nanosheets of the required size, with further enhancement in properties through combination with co-catalysts. Considering the wide bandgap of the DJ materials investigated in this study (3.45 eV) and the broad potential compositional space for DJ phases, their photocatalytic performance could be further improved in the future by engineering/identifying narrower bandgap compositions. Nitridation and doping with larger A-site cations may also effectively reduce the band gap energies as suggested in previous reports,[3] which would further improve photocatalytic performance of DJ phases, making them potentially excellent photocatalytic materials.

## Conflicts of interest

There are no conflicts to declare.

## Acknowledgements

Michael J. Reece and W. Xiong would like to thank EPSRC (MASSIVE, EP/L017695/1) for supporting this work. W. Xiong, J. Feng and H. Luo gratefully acknowledge the China Scholarship Council (CSC) for supporting their PhD studies.

## Notes and references

1 S. Ahmad, P. Fu, S. Yu, Q. Yang, X. Liu, X. Wang, X. Wang, X. Guo and C. Li, *Joule*, 2019, **3**, 794.
2 A. Fakharuddin, U. Shabbir, W. Qiu, T. Iqbal, M. Sultan, P. Heremans and L. Schmidt-Mende, *Adv. Mater.*, 2019, 1807095.
3 M. Hojamberdiev, M. F. Bekheet, E. Zahedi, H. Wagata, Y. Kamei, K. Yubuta, A. Gurlo, N. Matsushita, K. Domen and K. Teshima, *Cryst. Growth Des.*, 2016, **16**, 2302.
4 N. Kulischow, C. Ladasiu and R. Marschall, *Catal. Today*, 2017, **287**, 65.
5 T. Takata, K. Shinohara, A. Tanaka, M. Hara, J. N. Kondo and K. Domen, *J. Photochem. Photobiol., A*, 1997, **106**, 45.
6 B. W. Li, M. Osada, T. C. Ozawa and T. Sasaki, *Chem. Mater.*, 2012, **24**, 3111.
7 C. Chen, H. Ning, S. Lepadatu, M. Cain, H. Yan and M. J. Reece, *J. Mater. Chem. C*, 2015, **3**, 19.
8 M. Osada and T. Sasaki, *Adv. Mater.*, 2012, **24**, 210.
9 T. C. Ozawa, K. Fukuda, K. Akatsuka, Y. Ebina, T. Sasaki, K. Kurashima and K. Kosuda, *J. Phys. Chem. C*, 2008, **112**, 17115.
10 T. C. Ozawa, K. Fukuda, K. Akatsuka, Y. Ebina, T. Sasaki, K. Kurashima and K. Kosuda, *J. Phys. Chem. C*, 2008, **112**, 1315.
11 B.-W. Li, M. Osada, T. C. Ozawa, K. Akatsuka, Y. Ebina, R. Ma, K. Ono, H. Funakubo and T. Sasaki, *Jpn. J. Appl. Phys.*, 2010, **49**, 09MA01.
12 M. Osada, K. Akatsuka, Y. Ebina, H. Funakubo, K. Ono, K. Takada and T. Sasaki, *ACS Nano*, 2010, **49**, 5225.
13 R. E. Schaak and T. E. Mallouk, *Chem. Mater.*, 2002, **14**, 1455.
14 M. Osada and T. Sasaki, *Dalton Trans.*, 2018, **47**, 2841.
15 S. Ida, C. Ogata, U. Unal, K. Izawa, T. Inoue, O. Altuntasoglu and Y. Matsumoto, *J. Am. Chem. Soc.*, 2007, **129**, 8956.
16 B.-W. Li, M. Osada, Y.-H. Kim, Y. Ebina, K. Akatsuka and T. Sasaki, *J. Am. Chem. Soc.*, 2007, **139**, 10868.
17 N. A. Benedek, *Inorg. Chem.*, 2014, **53**, 3769.
18 R. Marschall, *Adv. Funct. Mater.*, 2014, **24**, 2421.
19 G. Liu, L. Ma, L. C. Yin, G. Wan, H. Zhu, C. Zhen, Y. Yang, Y. Liang, J. Tan and H. M. Cheng, *Joule*, 2018, **2**, 1095.
20 X. Zhou, J. Jankowska, H. Dong and O. V. Prezhdo, *J. Energy Chem.*, 2018, **27**, 637.
21 A. Chen, X. Zhang, Z.-H. Zhang, S. Yao and Z. Zhou, *J. Mater. Chem. A*, 2019, **7**, 11530.
22 Z.-Q. Zhang, L.-L. Bai, Z.-J. Li, Y. Qu and L.-Q. Jing, *J. Mater. Chem. A*, 2019, **7**, 10879.
23 W. S. Kuo, N. H. Tai and T. W. Chang, *Composites, Part A*, 2013, **51**, 56.
24 Y. Cui, J. Briscoe and S. Dunn, *Chem. Mater.*, 2013, **25**, 4215.
25 Y. Ebina, T. Sasaki, M. Harada and M. Watanabe, *Chem. Mater.*, 2002, **14**, 4390.
26 F. Chen, Z. Ren, S. Gong, X. Li, G. Shen and G. Han, *Chem.–Eur. J.*, 2016, **22**, 12160.
27 U. Khan, A. O'Neill, H. Porwal, P. May, K. Nawaz and J. N. Coleman, *Carbon*, 2012, **50**, 470.
28 M. Buzaglo, E. Ruse, I. Levy, R. Nadiv, G. Reuveni, M. Shtein and O. Regev, *Chem. Mater.*, 2017, **29**, 9998.

 